Journal of Statistical Physics, Vol. 82, Nos. 1/2, 1996

Molecular Dynamics Simulation of Size Segregation in Three Dimensions

Jason A. C. Gallas,[1,2] **Hans J. Herrmann,**[1,3]
Thorsten Pöschel,[1,4] **and Stefan Sokołowski**[1,5]

Received May 22, 1995

We report the first three-dimensional molecular dynamics simulation of particle segregation by shaking. Two different containers are considered: one cylindrical and another with periodic boundary conditions. The dependence of the time evolution of a test particle inside the material is studied as a function of the shaking frequency and amplitude, damping coefficients, and dispersivity.

KEY WORDS: Size segregation; molecular dynamics; granular dynamics; whale effect; granular materials.

Dynamical properties of mesoscopic materials such as grains and powders have been subjects of recent research, both theoretically and experimentally.[6] In spite of much work, relatively little is known about the basic physical processes involved in the dynamics of granular media and many puzzles remain to be solved in this field. Apart from posing numerous fundamental and difficult questions from a theoretical point of view, knowledge of granular dynamics is needed for many industrial applications involving the preparation of food, drugs, detergents, cosmetics, cements, etc. (see, e.g., ref. 2). Granular dynamics appears also during industrial processes such as the homogenization of plastic "pills" before melting them into, for example a compact disc, or in the development of new materials such as *transparent* ceramics, a process which involves careful powder compaction before sintering.[3] A common feature of all these processes is the

[1] Höchstleistungsrechenzentrum, Forschungszentrum Jülich, D-52425 Jülich, Germany.
[2] Instituto de Física da UFRGS, 91501-970 Porto Alegre, Brazil.
[3] Laboratoire de Physique des Milieux Hétérogènes, ESPCI, 75231 Paris, France.
[4] Humboldt-Universität zu Berlin, Institut für Theoretische Physik, D-10115 Berlin, Germany.
[5] Computer Laboratory, Faculty of Chemistry, MCS University, 20031 Lublin, Poland.
[6] The literature is vast. Recent surveys include those in ref. 1.

0022-4715/96/0100-0443$09.50/0

dynamical interplay of polydisperse granular particles. From the plethora of complex behaviors present in cohesionless polydisperse granular materials, this paper presents results of a full 3D molecular dynamics simulation of size segregation by shaking, the so-called "Brazil nuts" effect, the effect by which large particles move to the top when shaken or jostled (see, e.g., ref. 4). Size segregation has been discussed recently,[5-7] but difficulties with its theoretical description using variants of the sequential algorithm originally proposed by Visscher and Bolsterli[8] has led to some controversy.[9] Using molecular dynamics, the present paper reports results of the first 3D simulation of the problem. A basic result reported here is the qualitative reproduction of an effect that is trivial to observe experimentally: the up-and-down movement of large test particles immersed in the granular media. As far as we know, our simulation is the first one able to reproduce this simple and important bidirectional effect.

Several models describing inelastic collisions between noncohesive grains exist in the literature.[1, 10, 11] Here we use the same expressions as discussed by Walton[1] and Haff and Werner.[10] We have previously applied similar expressions to simulate a few different experiments,[7] always then in two dimensions. In the framework defined in refs. 1 and 10, grains are treated as polydisperse assemblies of spheres with translational and rotational degrees of freedom. Two grains i and j undergo an inelastic collision whenever the sum of their radii R_{ij} satisfies the relation $|\mathbf{r}_i - \mathbf{r}_j| < R_{ij}$ with $\mathbf{r}_i$ and $\mathbf{r}_j$ the center-of-mass positions of the grains. During collisions grains feel a contact force given by the sum of normal and shear components. The shear components also contribute to the total torques acting on the grains. The normal component is

$$\mathbf{N}_{ij} = \{ Y(R_{ij} - |\mathbf{r}_i - \mathbf{r}_j|)^{3/2} - \gamma_n m_{ij}(|\mathbf{v}_i - \mathbf{v}_j|) \cdot \mathbf{n}_{ij} \}\, \mathbf{n}_{ij}$$

where $Y = \mathscr{Y}/(1/R_i + 1/R_j)^{1/2}$ and $\mathscr{Y}$ is the Young modulus for collisions between grains of radii R_i and R_j.[16] Here γ_n is the damping constant along the normal $\mathbf{n}_{ij} = (\mathbf{r}_i - \mathbf{r}_j)/|\mathbf{r}_i - \mathbf{r}_j|$, $\mathbf{v}_i$ is the translational velocity, and $m_{ij} = m_i m_j/(m_i + m_j)$ is the ijth reduced mass. The intergranular shear force is

$$\mathbf{S}_{ij} = \{ \min(-\gamma_s m_{ij} V_{ij}, \mu\, |\mathbf{N}_{ij} \cdot \mathbf{n}_{ij}|) \}\, \mathbf{s}_{ij}$$

where V_{ij} is the magnitude of the relative surface velocity in the tangential direction defined by

$$\mathbf{V}_{ij} = \mathbf{v}_i - \mathbf{v}_j - [(\mathbf{v}_i - \mathbf{v}_j) \cdot \mathbf{n}_{ij}]\, \mathbf{n}_{ij} + R_i(\mathbf{r}_i - \mathbf{r}_j) \times \boldsymbol{\Omega}_i + R_j(\mathbf{r}_i - \mathbf{r}_j) \times \boldsymbol{\Omega}_j$$

[7] Convection,[12] fluidization,[13] transport on a vibrating belt,[14] nonspherical particles.[15]

γ_s is the damping coefficient in the shear direction, μ is the Coulomb frictional coefficient, $\mathbf{s}_{ij} = \mathbf{V}_{ij}/V_{ij}$ and Ω is the angular velocity. The torques acting on the grain i are $\mathbf{T}_i = \mathbf{r}_{ci} \times \mathbf{S}_{ij}$, where $\mathbf{r}_{ci} = \mathbf{r}_c - \mathbf{r}_i$, $\mathbf{r}_c$ is the position of the contact point for collisions with some grain j.

Two types of containers were investigated: one cylindrical and another rectangular, the latter with periodic boundary conditions along x and y directions. Simulations were done for 1000 small spheres with radii uniformly distributed between $0.5 \leqslant R_i \leqslant 1.0$ mm and a single big *test* sphere of radius R_{big}, typically 2.5 mm. Walls were built with particles of radii $R_w = 1$ mm smeared out over their full length, that is, whenever a particle reaches the borders, it feels the presence of a wall grain with radius R_w. Gravity $g = 10\ \text{m/s}^2$ was directed vertically along the z axis and both containers were vibrated according to $z(t) = A \sin(2\pi f t)$. As before,[12–15] equations of motion were solved using predictor-corrector techniques of fourth order for translational motions and fifth order for rotations.[17] Particles were assumed to have a constant density of $2\ \text{g/cm}^3$ and moments of inertia were evaluated from $0.4 m_i R_i^2$. The elastic property of the collisions was chosen to be $\mathscr{Y} = 10^7\ \text{g/(s}^2\ \text{m)}$. The damping coefficients were mostly $\gamma_n = 2500\ \text{s}^{-1}$ and $\gamma_s = 1000\ \text{s}^{-1}$, with corresponding parameters for particle–wall collisions being four times higher, including $\mathscr{Y}$. The Coulomb coefficient was always $\mu = 0.2$. Equations of motion were integrated using a time step of 5 μs. Thus, a time evolution of 1 s corresponds to integrating all 1001 equations of motion 2×10^5 times, a quite demanding task computationally. Not all numerical values defined above are those that one would like to use ideally in simulations. The Young modulus is rather low, the damping coefficients γ_n and γ_s are also relatively small, and grains are softer than those of, e.g., real sand. However, if one replaces these parameters by more realistic ones the timestep needed for integrations becomes prohibitively small and it is no longer possible to follow the dynamics over a reasonable time interval.

We start by presenting results for the cylindrical container (fixed boundary conditions). At $t = 0$ the big particle was placed at the center of the bottom of the container while the 1000 small particles were simultaneously released from random positions above. After equilibration the container was vibrated. Two main quantities were then recorded: z_{big}, the relative position of the big particle with respect to the bottom of the container, and

$$z_{\text{ave}} \equiv \frac{1}{N} \frac{1}{\tau} \sum_{i=1}^{N} \sum_{t=0}^{\tau} z_i(t)$$

the average position of the N small particles, averaged also over the

elapsed time interval τ. Positions and velocities of all particles were also recorded at determined time intervals and used as input for making a video animation of the simulation. Such real-time recordings are particularly helpful to determine adequate parameters and timestep for simulations. Figure 1 shows the time evolution of two groups of curves, z_{big} and z_{ave}, as a function of frequency. In this and subsequent figures, the number of layers was defined as the vertical coordinates divided by the average radius of the small particles, 0.75 mm. At low frequencies the big particle remains essentially on the bottom, i.e., there is no segregation; for intermediate frequencies it goes up and remains there. If the frequency is further increased, the test particle may eventually dive deeply back into the granular assembly. This effect has also been noted in experiments[18] and is a consequence of very strong and deep convection rolls that are established by the fixed walls of the container. This because as the frequency increases, the assembly is not as compact as before. A possible explanation for this behavior seems to be the relatively high dampings involved either between interparticle collisions or in collisions with the wall. While Fig. 1 seems to present strong evidence of size segregation, we must add that since it takes very long times to compute the dynamics, there is no guarantee that we have been able to reach steady-state behavior in all cases, although we believe we reached steady-state in the majority of experiments.

Figure 2 shows the dependence of the dynamics upon R_{big} for fixed frequency. Compared to Fig. 1, now one sees no swelling (i.e., z_{ave} are the same for all curves), since this effect is mainly due to changes in frequency.

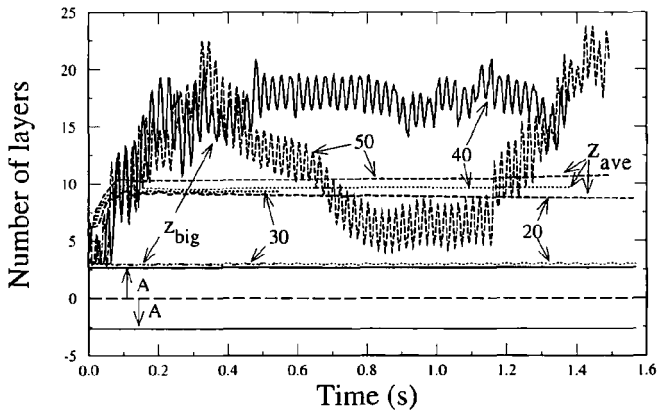

Fig. 1. Time evolution of the vertical coordinate z_{big} of a big particle with $R_{big} = 2.5$ mm and of z_{ave} inside a cylindrical container. Numbers are frequencies of vibration in Hz. Amplitude of oscillation is $A = 2$ mm.

The curve for $R_{big} = 2.5$ mm is the same as in Fig. 1. For slightly smaller radius the situation is less stable and the particle tends to stay within the upper one-third of the system. For $R_{big} = 1$ mm, the system has only small grains. In this case the test particle displays a diffusive motion inside the system. Changes in the dynamics due to different damping coefficients may be seen in Fig. 3. The situations labeled a and b correspond, respectively, to damping constants four and eight times smaller than those used in Fig. 1. We have performed additonal simulations for the same dampings as in Fig. 1 and found that altogether the dependence of segregation on damping coefficients is rather weak in this range of parameters. For each frequency there might be parameters at which segregation does occur anyway. For example, notice on the curve b some attempts of the probe to move upward when $f = 20$ Hz and the dissipation is 1/8 of the reference $\gamma_s = 1000$. Curve a appears to consist of a sequence of pulses with roughly constant amplitudes. As one easily recognizes from video recordings, trains (i.e., series of oscillations having similar amplitudes) with lower amplitude correspond to time intervals in which the probe is touching the wall. One important question that remains open is how the precise transition from "sitting on the bottom" to "moving upward" occurs. Notice that the probe could be going up very slowly, much slower than it is possible to recognize from the time scale of simulations presently feasible. Clarification of this point will certainly require further extensive computations.

We also made simulations using periodic boundary conditions, aiming to gain insight about behaviors that might exist for infinitely large systems. A salient difference of using periodic boundary conditions is that for

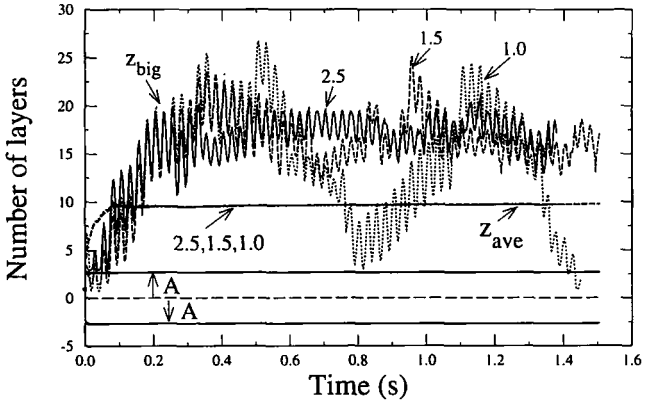

Fig. 2. Segregation as a function of the radius of the large particle (indicated by the numbers). In all cases $f = 40$ Hz and $A = 2$ mm. Numbers correspond to R_{big} in mm.

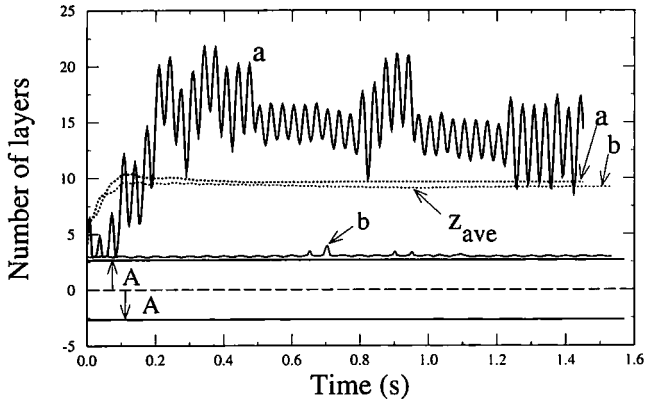

Fig. 3. Influence of the damping coefficients on the upward movement for (a) $f = 30$ Hz, $\gamma_n = 600$, and $\gamma_s = 250$, and (b) $f = 20$ Hz, $\gamma_n = 300$, and $\gamma_s = 125$. In both cases $R_{big} = 2.5$ mm and $A = 2$ mm.

frequencies and amplitudes where we previously found strong up-and-down motions of the large particle ("whale" effect), as seen in Fig. 1 for 50 Hz, for example, we now find a segregated state with the probe floating at the top of a number of layers in a less dense state. This is so because small convection cells appear localized only on the surface, yielding effectively some fluidized region only on the top. A steadystate with the probe at the top happens for frequencies around 20 Hz and amplitude 1 mm, a situation that might be realized experimentally with no difficulty. Without periodic boundary conditions the acceleration $\Gamma = 4\pi^2 f^2 A$ which characterizes the onset of fluidization[19] is $\Gamma^* = 15$ m/s^2, higher than gravity but much less than that with fixed walls (cylindrical geometry), which has $\Gamma = 2.25\Gamma^*$. One explanation for this difference seems to be the importance of the damping introduced by the cylindrical walls. About one-fifth of the total number of small particles touch the lateral wall. This means that energy is quite effectively damped at the walls. To assess the importance of the damping resulting from friction with the walls we performed another simulation, with results summarized in Fig. 4. This figure compares the dynamics as seen when using (a) a cylindrical cell without friction on the walls and (b) a cell with periodic boundary conditions. From this figure one sees that the dynamics without damping is essentially the same as that obtained when using periodic boundary conditions, a prediction it would be of interest to check experimentally.

In summary, for low frequencies there is no segregation. As the frequency rises we clearly find a "segregated regime" with the big particle essentially stable on the top. As the frequency increases beyond this regime

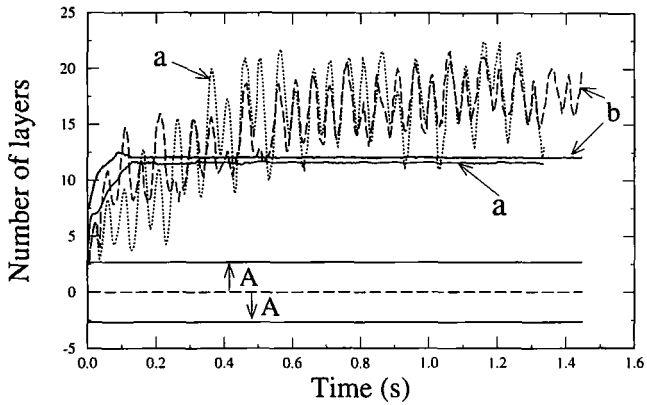

Fig. 4. A cylindrical container with frictionless lateral walls (a) and a container with periodic boundary conditions (b) display similar dynamics. Solid curves are z_{ave}, with corresponding noncontinuous curves displaying z_{big}. In both cases, $R_{big} = 2.5$ mm, $A = 2$ mm, and $f = 20$ Hz.

one sees the big particle dive inside the bulk. This is because the bulk is then not as "solid" as before. Our simulation correctly recovers several aspects that are seen in experiments and for which there was no previous theoretical description. Unfortunately, important questions such as the exact mechanism driving the segregation and the role of convection on the process cannot be easily assessed yet. They require a detailed investigation of the (rather large!) parameter space of the system. The factors limiting simulations of the real physical situation (and not caricatures of it) are the step size and the number of particles that one is able to consider, even when using some of the most powerful computational resources available today.

ACKNOWLEDGMENTS

We thank Stephan Melin for sharing with us his expertise with the AVS graphic package. H.J.H. is supported in part by the URA-CNRS 857 (France).

REFERENCES

1. O. R. Walton, in *Numerical simulation of inelastic, frictional particle-particle interactions*; M. C. Roco, ed. (Butherworth-Heinemann, Boston, 1992); S. B. Savage, in *Disorder and Granular Media*; D. Bideau, ed. (North-Holland, Amsterdam, 1992); H. M. Jaeger and S. Nagel, *Science* **255**:1532 (1992); A. Mehta, ed., *Granular Matter* (Springer, New York, 1994).

2. M. Poux *et al.*, *Powder Technol.* **68**:213 (1991).
3. A. Pechenik, G. J. Piermarini, and S. C. Danforth, *J. Am. Ceram. Soc.* **75**:3283 (1992); M. R. Gallas, B. Hockey, A. Pechenik, and G. J. Piermarini, *J. Am. Ceram. Soc.* **77**:2107 (1994); M. R. Gallas and G. J. Piermarini, *J. Am. Ceram. Soc.* **77**:2917 (1994).
4. A. Rosato, K. J. Strandburg, F. Prinz, and R. H. Swendsen, *Phys. Rev. Lett.* **58**:1038 (1987); *Powder Technol.* **49**:59 (1986); P. Devillard, *J. Phys. France* **51**:369 (1990).
5. J. B. Knight, H. M. Jaeger, and S. R. Nagel, *Phys. Rev. Lett.* **70**:3728 (1993).
6. J. Duran, J. Rajchenbach, and E. Clement, *Phys. Rev. Lett.* **70**:1405 (1993).
7. R. Jullien, P. Meakin, and A. Pavlovitch, *Phys. Rev. Lett.* **69**:640 (1992).
8. W. M. Visscher and M. Bolsterli, *Nature* **239**:504 (1972).
9. G. C. Barker, A. Mehta, and M. J. Grimson, *Phys. Rev. Lett.* **70**:2194 (1993).
10. P. K. Haff and B. T. Werner, *Powder Technol.* **48**:239 (1986).
11. C. S. Campbell, *Annu. Rev. Fluid Mech.* **22**:57 (1990).
12. J. A. C. Gallas, H. J. Herrmann, and S. Sokołowski, *Phys. Rev. Lett.* **69**:1371 (1992).
13. J. A. C. Gallas, H. J. Herrmann, and S. Sokołowski, *Physica A* **189**:437 (1992).
14. J. A. C. Gallas, H. J. Herrmann, and S. Sokołowski, *J. Phys. II* (Paris) **2**:1389 (1992).
15. J. A. C. Gallas and S. Sokołowski, *Int. J. Mod. Phys. B* **7**:2037 (1993).
16. L. D. Landau and E. M. Lifschitz, *Elastizitätstheorie*, 7th ed. (Akademie Verlag, Berlin, 1991).
17. M. P. Allen and D. J. Tildesley, *Computer Simulation of Liquids* (Oxford University Press, Oxford, 1987).
18. J. Duran, Private communication.
19. P. Evesque and J. Rajchenbach, *Phys. Rev. Lett.* **62**:44 (1989).

Communicated by D. Stauffer